Molecular Therapy
Original Article

Safe Recombinant Outer Membrane Vesicles that Display M2e Elicit Heterologous Influenza Protection

Hannah C. Watkins,[1] C. Garrett Rappazzo,[1] Jaclyn S. Higgins,[2] Xiangjie Sun,[3] Nicole Brock,[3] Annie Chau,[2] Aditya Misra,[4] Joseph P.B. Cannizzo,[5] Michael R. King,[1] Taronna R. Maines,[3] Cynthia A. Leifer,[6] Gary R. Whittaker,[6] Matthew P. DeLisa,[4] and David Putnam[1,4]

[1]Meinig School of Biomedical Engineering, Cornell University, Ithaca, NY 14853, USA; [2]Department of Biological and Environmental Engineering, Cornell University, Ithaca, NY 14853 USA; [3]Influenza Division, National Center for Immunization and Respiratory Diseases, Centers for Disease Control and Prevention, Atlanta, GA 30333, USA; [4]Smith School of Chemical and Biomolecular Engineering, Cornell University, Ithaca, NY 14853, USA; [5]College of Agriculture and Life Sciences, Cornell University, Ithaca, NY 14853, USA; [6]Department of Microbiology and Immunology, Cornell University College of Veterinary Medicine, Ithaca, NY 14853, USA

Recombinant, *Escherichia coli*-derived outer membrane vesicles (rOMVs), which display heterologous protein subunits, have potential as a vaccine adjuvant platform. One drawback to rOMVs is their lipopolysaccharide (LPS) content, limiting their translatability to the clinic due to potential adverse effects. Here, we explore a unique rOMV construct with structurally remodeled lipids containing only the lipid IVa portion of LPS, which does not stimulate human TLR4. The rOMVs are derived from a genetically engineered B strain of *E. coli*, ClearColi, which produces lipid IVa, and which was further engineered in our laboratory to hypervesiculate and make rOMVs. We report that rOMVs derived from this lipid IVa strain have substantially attenuated pyrogenicity yet retain high levels of immunogenicity, promote dendritic cell maturation, and generate a balanced Th1/Th2 humoral response. Additionally, an influenza A virus matrix 2 protein-based antigen displayed on these rOMVs resulted in 100% survival against a lethal challenge with two influenza A virus strains (H1N1 and H3N2) in mice with different genetic backgrounds (BALB/c, C57BL/6, and DBA/2J). Additionally, a two-log reduction of lung viral titer was achieved in a ferret model of influenza infection with human pandemic H1N1. The rOMVs reported herein represent a potentially safe and simple subunit vaccine delivery platform.

INTRODUCTION

There is high demand for tailored vaccine adjuvants that can elicit directed immune responses against protein-based antigens.[1] Traditionally, vaccines are made from inactivated or live attenuated pathogens. Although inactivated and live attenuated vaccines often offer the longest immune memory and protection, they are not suitable for all pathogens due to safety concerns, such as the possibility of reversion and contraindications for use in immune-compromised patients. Recombinant subunit vaccines and virus-like particles (VLPs) are attractive alternative design choices, as they induce immunity to pathogen-derived antigens in the absence of the pathogen itself. However, unlike inactivated or live attenuated vaccines, which retain inherent immunogenicity from the pathogen, recombinant subunit vaccines often require an adjuvant to generate a sufficient immune response and to appropriately direct the immune system.[2] Recombinant *Escherichia coli*-derived outer membrane vesicles (rOMVs) are a naturally self-adjuvanting and unique pathogen mimetic vaccine platform that represent a link between inactivated vaccines and subunit vaccines. rOMVs are shed from hypervesiculating strains of *E. coli*, resulting in vesicles that contain pathogen-associated molecular patterns (PAMPs) but are noninfectious,[3,4] The hypervesiculating *E. coli* strains are transformed with a plasmid encoding an antigen of interest genetically fused to a transmembrane protein, resulting in antigen transport to the outer membrane of *E. coli* and subsequent display on rOMVs.[5] Previously, rOMV vaccines proved capable of generating strong immune responses to antigens of interest displayed on their surface and in inducing protection against bacterial and viral pathogens, demonstrating their potential as a vaccine platform.[6–9]

Although rOMV-based vaccine platforms show significant promise, their lipopolysaccharide (LPS) content hampers clinical translation.[10,11] LPS is a potent adjuvant that stimulates through Toll-like receptor 4 (TLR4), but high levels can lead to fever, inflammation, and septic shock.[12] Modification to the lipid A region of LPS can greatly impact its ability to interact with TLR4 and increases the safety of LPS as an adjuvant. *lpxM* knockout *E. coli* strains, which produce pentacylated LPS instead of hexacylated LPS, were previously used to generate rOMVs with attenuated LPS toxicity.[6,13,14] However, rOMVs containing only the LPS precursor lipid IVa, which is a human TLR4 antagonist, have not yet been tested immunologically,

Received 2 June 2016; accepted 6 January 2017;
http://dx.doi.org/10.1016/j.ymthe.2017.01.010.

Correspondence: David Putnam, 147 Weill Hall, 526 Campus Road, Cornell University, Ithaca, NY 14853, USA.
E-mail: dap43@cornell.edu

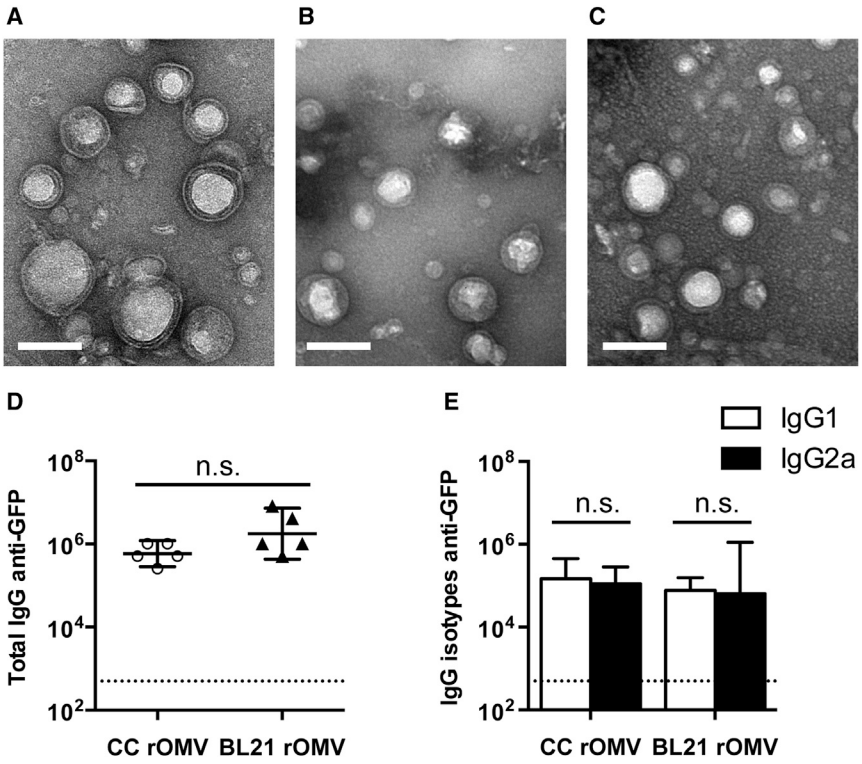

Figure 1. rOMVs Produced from Three Different *E. coli* Strains Are Structurally Comparable

(A–C) TEM images of rOMVs stained with uranyl acetate: CC rOMVs (A), BL21 rOMVs (B), and Nsl rOMVs (C). Scale bars represent 100 nm. (D and E) Total IgG (D) and isotypes IgG1 and IgG2a (E) anti-GFP titers from BALB/c mice 8 weeks post prime dose of ClyA-GFP-expressing CC or BL21 rOMVs. Titer error bars represent 95% confidence intervals (CI) of geometric mean. Log-transformed data analyzed using an unpaired Student's t test to compare CC versus BL21 rOMV anti-GFP IgG levels and using paired Student's t test to compare IgG1:IgG2a levels for each rOMV type. Dotted line indicates titer of sera from mice pre-vaccination.

although they were recently used as a method for determining the mechanism of polysaccharide conjugation in *E. coli*.[15] Unlike LPS, lipid IVa is an antagonist to human TLR4, although it does still retain some ability to stimulate murine TLR4.[16] The *E. coli* strain, BL21(DE3) (BL21), was recently engineered to contain only lipid IVa instead of full LPS. This strain, KPM404, sold as ClearColi (CC), is marketed by Lucigen as an endotoxin-free *E. coli* strain for use in recombinant protein production.[17] Despite containing only lipid IVa, we hypothesized that CC-derived rOMVs would retain sufficient intrinsic PAMPs to generate equivalent immunity against displayed exogenous proteins, but with greatly reduced pyrogenicity and toxicity when compared to LPS-unmodified rOMVs.

Here, we report a retooling of the rOMV adjuvant platform that significantly reduces endotoxicity while maintaining adjuvant potential, thereby opening the opportunity of rOMVs to translate into the clinic. We engineered CC to hypervesiculate and compared the ability of CC rOMVs versus the parent strain BL21-derived rOMVs to trigger immune responses both in vivo and in vitro. Additionally, we directly compared the immune responses of CC rOMVs to *E. coli* Nissle 1917 (Nsl) rOMVs, which previously demonstrated superior immunomodulatory properties relative to rOMVs derived from *E. coli* K12 strains.[6] Finally, we evaluated the efficacy of CC rOMVs to protect against influenza challenge in mice of three genetic backgrounds (BALB/c, C57BL/6, and DBA/2J) as well as in the more clinically relevant ferret model against human pandemic H1N1 influenza. Collectively, our results demonstrate that CC rOMVs offer significantly improved safety over other rOMV *E. coli* source strains investigated herein, and maintain the rOMV benefits of potent immune responses.

RESULTS

Antigen Expressing ClearColi and BL21 rOMVs Produce and Display Equivalent In Vivo Immunogenicity

CC and its parent strain, BL21(DE3), were engineered to hypervesiculate through knockout of *nlpI*, which is known to induce increased vesiculation in laboratory strains of *E. coli*.[18,19] rOMVs were imaged using transmission electron microscopy (TEM) and demonstrated similar morphology and size (50–100 nm) to rOMVs produced by the previously reported *E. coli* strain Nissle 1917 (Nsl) (Figures 1A–1C).[10] CC and BL21 were further modified by transformation with plasmids carrying the gene for transmembrane protein cytolysin A (ClyA) fused to GFP.[5] Western blot confirmed that the rOMVs contained ClyA-GFP (Figure S1A).

To provide a direct assessment of the role LPS plays in eliciting a humoral response against rOMV displayed proteins, 10-week-old BALB/c mice were injected with 20 μg of ClyA-GFP displaying rOMVs (containing ~0.4 μg of GFP) derived from either CC (n = 5) or BL21 (n = 5), and then given an equivalent boost dose 4 weeks later. Humoral immune response to the rOMV vaccines was evaluated using serum from 8 weeks post-prime injection and measuring the anti-GFP titers of total IgG and IgG isotypes. Both CC and BL21 ClyA-GFP rOMV-vaccinated mice developed high total IgG titers, and the geometric mean of anti-GFP titers elicited by CC did not vary significantly from those elicited by BL21 ($p > 0.05$) (Figure 1D). The serum was further analyzed for IgG1 and IgG2a isotype titers to assess immune system bias and found a balanced IgG1:IgG2a ratio generated by both CC and BL21 rOMVs (Figure 1E). Therefore, although the CC rOMVs contained only lipid IVa, they were able to elicit a strong anti-GFP humoral immune response that was equivalent to that of their parent strain, BL21, which contained unmodified LPS.

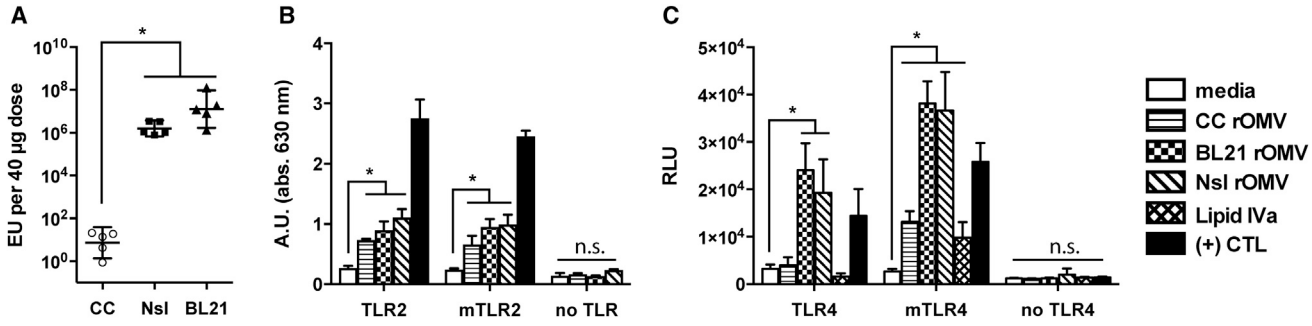

Figure 2. Pyrogenicity and TLR Activity Are rOMV Source Strain Dependent

(A) Pyrogenicity (measured in endotoxin units) of CC, Nsl, and BL21 rOMVS determined using whole-blood pyrogenicity test. Groups were compared with Kruskal-Wallis test, followed by Mann-Whitney between pairs, using Bonferroni method to account for multiple comparisons (*$p < 0.01$). Error bars represent 95% CI of geometric mean (n = 5 blood donors). (B) HEK-Blue KD-TLR5 cells transfected with human TLR2 or mTLR2 were stimulated with rOMVs (100 ng/mL) or Pam3Cys (1 µg/mL, (+) CTL) for 16 hr. (C) HEK-Blue KD-TLR5 cells transfected with 5x NF-κB-luciferase reporter and TLR4/MD-2/CD14 or mTLR4/mMD-2/mCD14 were stimulated with rOMVs (100 ng/mL), lipid IVa (100 ng/mL), or LPS (100 ng/mL, (+) CTL) for 16 hr. Samples analyzed by ANOVA followed by multiple comparisons against media using Dunnett method of correction (*$p < 0.0001$). Error bars represent SD (n = 4).

ClearColi-Derived rOMVs Have Greatly Reduced Pyrogenicity Compared to Parent Strain rOMVs

The investigational aim for CC rOMVs was to reduce the toxicity associated with high doses of rOMVs, while retaining the benefits of a pathogen mimetic particle. As CC rOMVs displayed equivalent capability to BL21 in generating anti-GFP titers, we sought to determine whether CC rOMVs had significantly reduced pyrogenicity relative to rOMVs derived from BL21 or Nsl strains using a whole-blood pyrogenicity test. In this test, the response of blood monocyte interactions with pyrogens is quantified by IL-1β release, which is then related to a standard endotoxin curve.[20] Thus, the readout for the whole-blood pyrogen test is endotoxin units (EU), although the test measures all pyrogens present and not just endotoxin (LPS). This test is performed using human blood, as humans have enhanced endotoxin and pyrogen sensitivity relative to mice.[21] CC rOMVs generated a response that was 10^5- to 10^6-fold lower than BL21 rOMVs and Nsl rOMVs, highlighting the impact that lipid IVa, as opposed to full LPS, has on reducing the overall toxicity (Figure 2A). Pure lipid IVa at a concentration of 10 µg/mL generated a response that was beneath detection by the IL-1β ELISA, confirming that it alone is not pyrogenic. Additionally, when PBS-suspended CC rOMVs were centrifuged a second time, and the supernatant was collected, the supernatant contained negligible pyrogen levels, indicating that it was the CC rOMVs driving the pyrogenicity and not dissolved factors in the supernatant. The assay highlights that, although CC rOMVs have significantly reduced pyrogenicity compared to other OMV types, they are not completely pyrogen free.

ClearColi rOMVs Stimulate through TLR2

The ability of CC rOMVs to generate equivalent immune titers as BL21 rOMVs led us to investigate their ability to trigger pathogen recognition receptors (PRRs) other than TLR4, of which LPS is a known agonist. First, rOMVs were used to stimulate a panel of TLR-transfected reporter cells. If CC rOMVs activate a particular TLR, it will result in activation of NF-κB. Cells transfected with TLR4 were also always transfected with species-specific essential co-factors MD-2 and CD14. Both murine (m) and human TLRs were tested (Figures 2B, 2C, and S2A–S2C). As expected, Nsl rOMVs signaled predominantly through murine and human TLR2 and TLR4, human TLR5, and murine TLR11, as was previously described.[10] BL21 rOMVs also stimulated TLR2 and TLR4; however, BL21 lack flagellin and thus did not stimulate TLR5 (Figures 2B, 2C, and S2A–S2C).[22] Similar to BL21, CC also does not make flagellin and lacks activity against TLR5 (Figure S2C). Unlike Nissle and BL21, CC showed no activity for human TLR4 (Figure 2C). CC did stimulate murine TLR4, although to a level significantly lower than either the BL21 or Nsl rOMVs. This is unsurprising, as it is reported that lipid IVa is a moderate agonist of murine TLR4, but an antagonist of human TLR4.[23,24] CC exhibited activity against both murine and human TLR2, indicating TLR2 stimulation might contribute to CC pyrogenicity (Figure 2B). None of the rOMVs showed activity against any of the other tested murine or human TLRs (Figures S2A and S2B). Nucleotide-binding oligomerization domain (NOD) receptors are intracellular sensors of bacteria, which detect motifs found in peptidoglycan.[25] Neither CC nor BL21 rOMVs caused a response in NOD1 or NOD2 reporter cells (Figures S2D and S2E). Although Nsl rOMVs did stimulate NOD1 and NOD2, the NOD1 and NOD2 reporter cell lines endogenously express TLR5, indicating that flagellin was possibly responsible for their activation. Although possible that CC rOMVs stimulate PRRs that were not tested, the data suggest that the immunogenicity of CC rOMVs is likely driven primarily by their TLR2 agonist activity.

ClearColi rOMVs Promote Dendritic Cell Maturation

Dendritic cells (DCs) play a key role in directing the immune system and help to facilitate bias toward a T helper 1 (Th1)- or Th2-type response.[26] Production of IL-12p70 by DCs triggers production of interferon γ (IFN-γ) by Th1 cells, cytotoxic T cells, and natural killer (NK) cells.[27] It is well established that LPS matures DCs and promotes a Th1 bias; therefore, we next asked whether the outer membrane

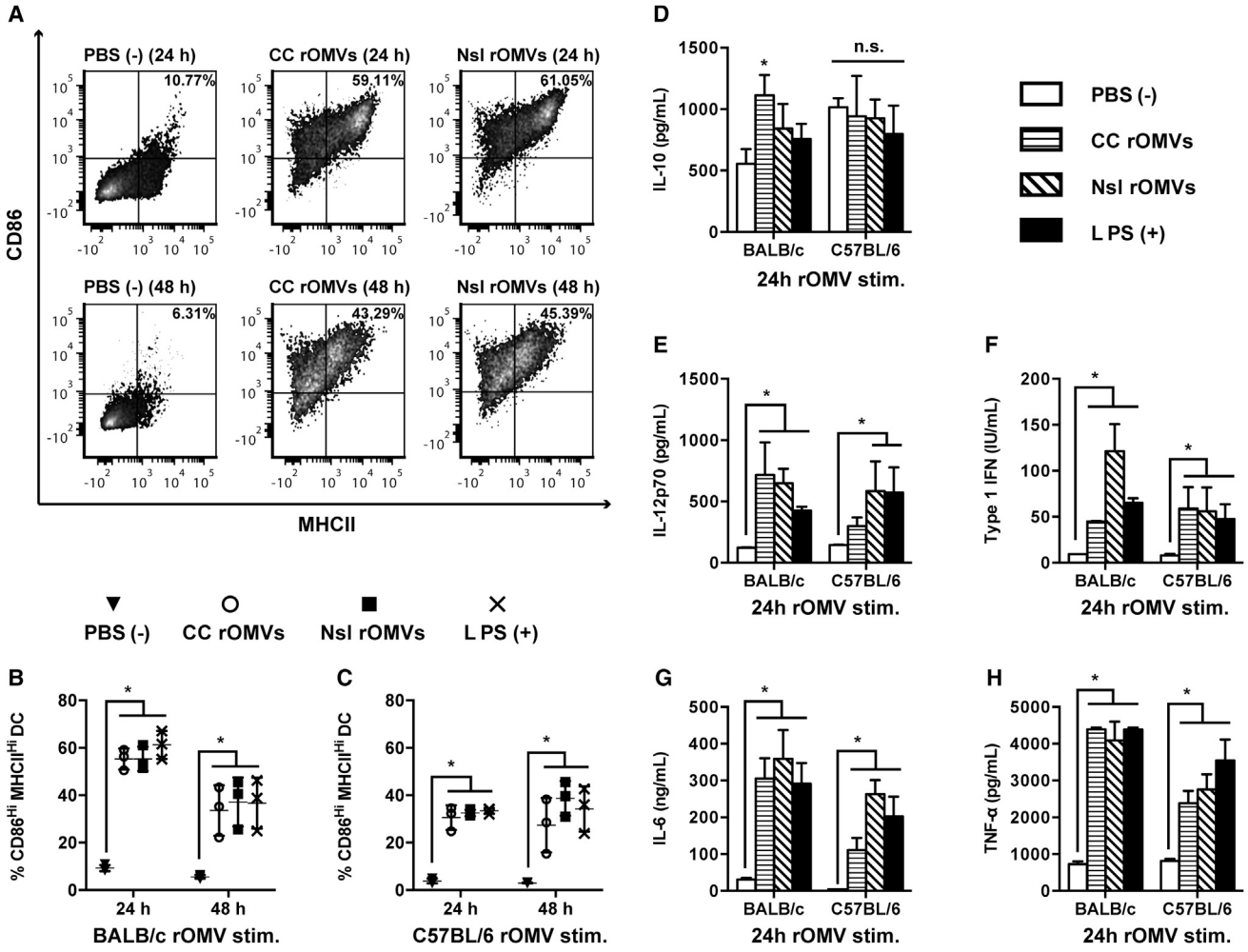

Figure 3. Bone Marrow-Derived Dendritic Cells Are Activated by rOMVs

Murine BMDCs from BALB/c and C57BL/6 mice were stimulated with NsI rOMVs (100 ng/mL), CC rOMVs (100 ng/mL), LPS (100 ng/mL), or PBS for 24 or 48 hr, then supernatants were collected for cytokine analysis, and cells were stained for DC maturation markers (stains: viability, CD11c, CD86, MHCII). Flow cytometry was used to determine percent mature dendritic cells (DCs) ($CD86^{Hi}$, $MHCII^{Hi}$) out of the total DC population (gated on viability, $CD11c^{Hi}$). (A) Representative density plots of BMDCs isolated from a BALB/c mouse. (B) Percent mature DCs from BALB/c mice. (C) Percent mature DCs from C57BL/6 mice. (D) IL-10 concentration after 24-hr stimulation. (E) IL-12p70 concentration (conc.) after 24-hr stimulation. (F) Type 1 IFN conc. after 24-hr stimulation. (G) IL-6 conc. after 24-hr stimulation. (H) TNF-α conc. after 24-hr stimulation. Cytokine stimulation is shown for both C57BL/6 and BALB/c mice. Error bars represent SD. Samples analyzed via ANOVA followed by Holm multiple-comparison test, *$p < 0.05$ ($n = 3$ mice).

composition of the lipid IVa-containing CC rOMVs could lead to maturation of DCs.[28] We compared the cytokines produced from bone marrow-derived dendritic cells (BMDCs) stimulated by CC and NsI rOMVs to determine whether one rOMV type was more prone to eliciting a Th1 bias. We focused our comparison on CC rOMVs versus NsI rOMVs, as there is precedent for NsI rOMVs being used in protective rOMV vaccines.[6,10] Immature BMDCs from BALB/c or C57BL/6 mice were incubated with CC rOMVs, NsI rOMVs, LPS (positive control), or PBS (negative control) for 24 or 48 hr. Both CC rOMVs and NsI rOMVs resulted in significant and equivalent BMDC maturation in both BALB/c and C57BL/6 mice, as indicated by upregulation of maturation markers CD86 and MHCII (Figures 3A–3C). Supernatants from the stimulated and unstimulated BMDCs were collected and measured for IL-10, IL-12p70, type 1 IFN, IL-6, and tumor necrosis factor α (TNF-α) (Figures 3D–3H and S3A–S3F). Production of IL-12p70 is associated with a Th1-biased inflammatory response, whereas production of IL-10 is associated with a suppressive immune response.[29] Treating BMDCs with rOMVs did not increase IL-10 production relative to the control PBS-treated cells, except in the 24-hr time point of BALB/c BMDCs treated with CC rOMVs. However, by 48 hr, the difference in IL-10 levels between PBS and CC rOMV-treated BALB/c BMDCs was no longer significant (Figure S3A). This observed decrease in IL-10 production suggests sustained BMDC activation at 48 hr, as mature

BMDCs lose sensitivity to IL-10 signaling.[30] IL-12p70 levels were significantly elevated after treatment with both CC and Nsl rOMVs in BALB/c mice but were significantly elevated only after treatment with Nsl rOMVs in C57BL/6 mice. CC rOMV treatment of C57BL/6 BMDCs did result in an increase in IL-12p70 production, but the difference was not significant. As expected, treatment with LPS led to significant production of IL-12p70 in BMDCs from both mouse strains. Analysis of type 1 IFN, IL-6, and TNF-α at 24-hr post-stimulation showed significant increases occurred after treatment with both CC rOMVs and Nsl rOMVs in both BALB/c and C57BL/6 mouse strains (Figures 3F–3H). The presence of type 1 IFN and TNF-α provide further confirmation of BMDC maturation, as type 1 IFNs have an activating effect on immature, committed dendritic cells by stimulating the upregulation of cell surface proteins MHCII and CD86.[31] Additionally, autocrine TNF-α has been shown to be necessary for the activation of BMDCs and survival of matured BMDCs.[32,33] Although the inflammatory properties of IL-6 are context dependent, IL-6 is known to have a significant role in promoting and directing the adaptive immune response. IL-6 induces B cell maturation into antibody-secreting cells and promotes the proliferation and survival of $CD4^+$ T cells.[34] Overall, the equivalent levels of BMDC maturation and increased levels of IL-12p70, IL-6, type I IFN, and TNF-α production, indicate potent immune activation. Only subtle differences were seen between mouse strains, indicating that rOMV vaccines should activate DCs in both Th2-biased BALB/c mice as well as Th1-biased C57BL/6 mice. Furthermore, the presence of lipid IVa instead of full LPS in CC rOMVs did not impair their ability to mature and activate dendritic cells.

ClearColi rOMVs Expressing Influenza A Antigen M2e4xHet Elicit High Titers without Side Effects in Mice

The CC rOMVs containing model antigen GFP demonstrated the ability to elicit high total IgG anti-GFP titers and in vitro work showed this was likely due to TLR2 stimulation, leading to DC maturation and immune-directive cytokine secretion. With these promising results, we sought to test the protective efficacy of the CC rOMV platform by creating CC rOMVs that displayed an influenza A-based peptide, M2e4xHet, fused to ClyA. The antigen M2e4xHet contains four variants of the influenza A virus matrix 2 protein separated by glycine/serine linkers (peptide sequence: SLLTEVETPIRNEWGSRSNDSSDgggsgggSLLTEVETPTRSEWESRSSDSSDgggsgggSLLTEVETPTRNEWESRSSDSSDgggsgggSLLTEVETLTRNGWGSRSSDSSD).[10] Western blot confirmed that the rOMVs contained the ClyA-M2e4xHet protein (Figure S1B). Previously, Nsl rOMVs displaying ClyA-M2e4xHet led to 100% protection from challenge with influenza A/Puerto Rico/8/1934 (PR8) (H1N1).[10] Thus, by comparing Nsl and CC M2e4xHet rOMVs, it is possible to determine whether CC rOMVs are as effective as an established rOMV vaccine in eliciting titers and providing influenza protection.

Seven-week-old BALB/c mice were immunized with 40 μg of CC M2e4xHet rOMVs (~2.4 μg of M2e4xHet), 40 μg of Nsl M2e4xHet rOMVs (~2.4 μg of M2e4xHet), or PBS. Following prime and boost immunization, mice were weighed daily for 1 week to determine whether the pyrogenicity of the rOMVs was causing negative side effects leading to weight loss (Figures 4A and 4B). Twenty-four hours post-vaccination, marked differences were seen between mice vaccinated with Nsl rOMV and CC rOMVs; Nsl rOMV-vaccinated mice exhibited anorexia, lethargy, and piloerection, whereas CC rOMV-vaccinated mice maintained normal activity and appearance. Mice vaccinated with Nsl rOMVs lost a similar amount of weight after both prime (Figure 4A) and boost (Figure 4B) doses, whereas mice vaccinated with CC rOMVs experienced no weight loss after either dose, and had an equivalent response to mice receiving sham PBS injections. The lack of negative side effects in CC rOMV-vaccinated mice versus Nsl rOMV-vaccinated mice emphasizes the increased safety profile of the CC rOMV vaccine.

Eight weeks following the prime vaccine dose, anti-M2e titers were measured to assess humoral vaccine response. Both CC and Nsl rOMVs generated high and equivalent total IgG anti-M2e titers ($p > 0.05$), indicating potential for both to be used as vaccine adjuvants (Figure 4C). Nsl rOMVs had slight, but significant ($p < 0.05$), elevation of IgG2a over IgG1 titers, whereas CC rOMVs resulted in a more balanced IgG2a:IgG1 response (Figure 4D). Although CC rOMVs did not lead to elevated IgG2a:IgG1 ratio, the geometric mean IgG2a titer of CC rOMV-vaccinated mice was not significantly different from that of Nsl rOMV-vaccinated mice ($p > 0.05$). The equivalent anti-M2e total IgG titers generated by Nsl and CC rOMVs once again demonstrate that full LPS is not necessary for CC rOMVs to cause a robust humoral immune response.

ClearColi M2e4xHet rOMVs Protect against Lethal Influenza A Challenge in BALB/c Mice

Ten weeks post-prime immunization, mice were challenged with a lethal dose (50 fluorescent forming units [FFU]) of influenza A strain PR8. In addition to the rOMV-vaccinated groups and the negative control group, which was administered PBS, a positive control group of pre-exposed mice was included. The pre-exposed mice were given a low dose (5 FFU) of PR8 virus 8 weeks prior to the lethal (50 FFU) dose, to allow them to develop a protective immune response against PR8. As expected, 100% of pre-exposed mice survived (five of five) and 0% of PBS-vaccinated mice survived (zero of five) (Figure 4E). Mice immunized with rOMVs from both Nsl and CC were equally protected: 80% of mice vaccinated with Nsl M2e4xHet rOMVs survived (four of five), and 100% of mice vaccinated with CC M2e4xHet rOMVs survived (five of five) (Figure 4E). Although one mouse in the Nsl rOMV group required euthanasia due to weight loss exceeding 30% original body weight, the survival of mice vaccinated with Nsl and CC rOMVs was statistically equivalent. The CC rOMV-vaccinated mice showed reduced morbidity with respect to the PBS negative control group and had weight loss that was statistically equivalent to the weight loss of the pre-exposed mice throughout the duration of the trial (Figure 4F). Although the literature suggests a Th1 bias is preferred for M2e-based vaccines, as IgG2a antibodies are a correlate of protection, the balanced CC rOMV vaccine response generated sufficient IgG2a to elicit full protection from challenge.[35,36] The 100% survival of BALB/c mice vaccinated with CC M2e4xHet rOMVs

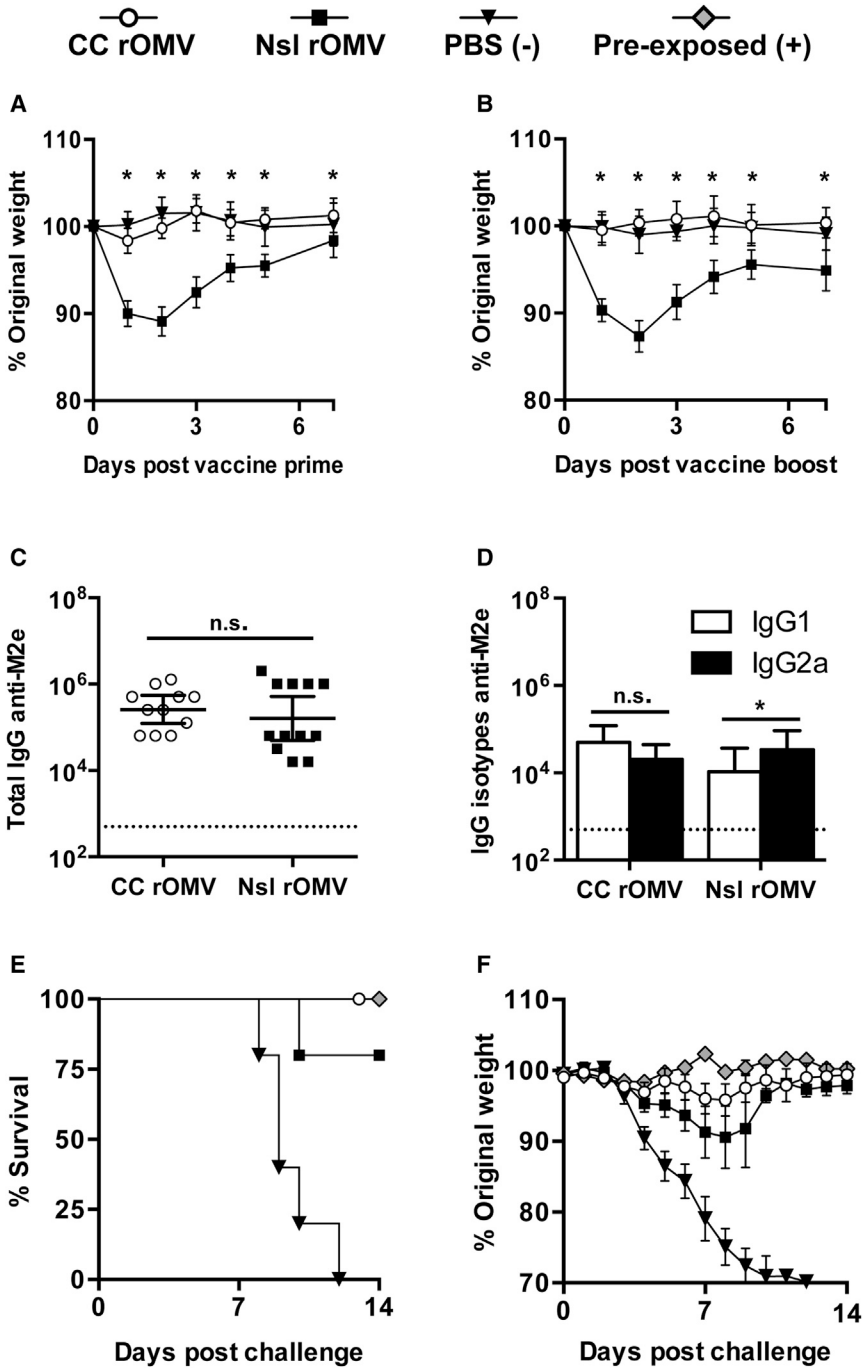

Figure 4. rOMV Source Strain Dependence on Morbidity, Immune Response, and Mortality

(A and B) Mice were weighed daily for 1 week post-prime (A) and boost (B) immunization. Analyzed using ANOVA followed by multiple comparisons using Dunnett method of correction. Error bars represent SD of mean (*$p < 0.001$). (C and D) Total IgG (C) and IgG isotypes IgG1 and IgG2a (D) anti-M2e titers of BALB/c mice 8 weeks post-prime rOMV immunization. Dotted line indicates lowest titer detectable above background (serum from PBS-vaccinated mice). Log-transformed IgG1 and IgG2a anti-M2e titers compared using paired t test. Error bars indicate 95% CI of geometric mean (*$p < 0.05$) (n = 11 CC rOMV-vaccinated mice, n = 12 NsI rOMV-vaccinated mice, n = 16 PBS-vaccinated mice). (E and F) Mortality (E) and weight loss (F) of mice challenged with a lethal dose (50 FFU) of influenza A/PR8 (n = 5 CC rOMV vaccinated, n = 5 NsI rOMV vaccinated, n = 5 PBS vaccinated, n = 5 pre-exposed). Kaplan-Meier survival curves were analyzed with a log-rank test using the Bonferroni method to account for multiple comparisons. Error bars on morbidity curves represent SEM.

demonstrates that the immune response elicited by CC rOMVs is protective against lethal influenza challenge.

ClearColi M2e4xHet rOMVs Elicit Th1 Bias in C57BL/6 Mice and Protect against Influenza Infection

Although previous studies have demonstrated protection against influenza using M2e-based antigens in BALB/c mice, fewer have assessed M2e-based antigens in C57BL/6 mice.[37–39] When Misplon et al. directly compared the response of BALB/c and C57BL/6 mice to M2e-based vaccines, they found significantly lower antibody and T cell responses in C57BL/6 mice.[40] Thus, to determine the robustness of the M2e4xHet antigen, and ability of CC rOMVs to adjuvant in varied mouse strains, ten C57BL/6 mice were given prime and boost doses of CC rOMVs containing the M2e4xHet antigen. Mouse weight was tracked for 3 days post-injection, but no weight loss or other side effects (lethargy, piloerection) were noted. Four weeks post-boost injection, blood was collected, and anti-M2e titers were assessed. The anti-M2e total IgG titers were high and statistically equivalent to those developed by the BALB/c vaccinated mice (Figure 5A). In contrast to the BALB/c mice, which developed a balanced IgG2a:IgG1 ratio, the C57BL/6 mice had significantly higher IgG2c titers than IgG1—several of the mice even had IgG1 levels that were beneath the limit of detection of the ELISA (Figure 5A). IgG2c levels were measured instead of IgG2a, as C57BL/6 mice do not produce IgG2a and instead produce IgG2c.[41] The mice were challenged at 10 weeks post-prime dose with a lethal dose of PR8 (100 FFU), which resulted in 100% survival of vaccinated mice and 0% survival of unvaccinated mice (Figure 5B). Although all CC rOMV-vaccinated mice survived, they did have significant weight loss compared to the positive control pre-exposed mice, which were exposed to a sublethal dose of PR8 (5 FFU) prior to receiving a lethal dose of PR8

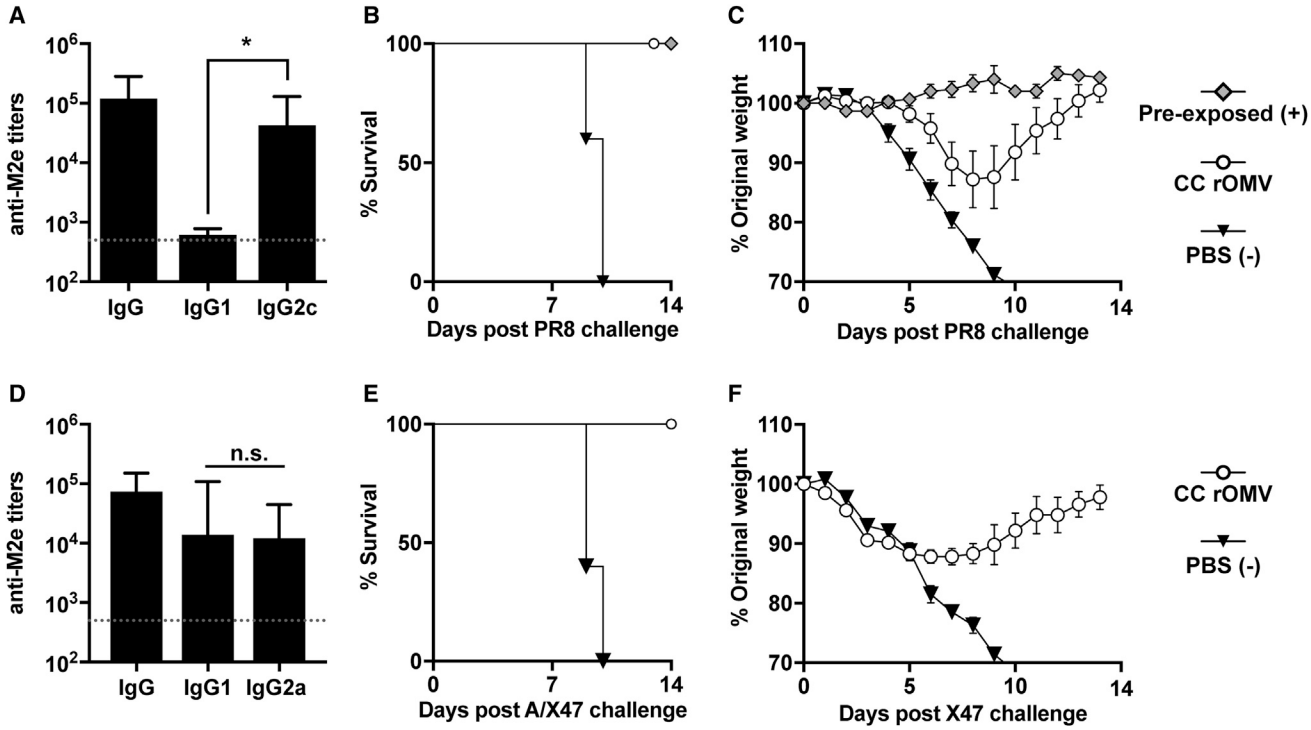

Figure 5. Immune Response, Mortality, and Morbidity in C57BL/6 and DBA/2J Mice

(A) Total IgG and isotypes IgG1 and IgG2c titers of C57BL/6 mice 8 weeks post-prime rOMV vaccination. Dotted line indicates lowest titer detectable above background. Log-transformed IgG1 and IgG2c titers compared using paired t test. Error bars indicate 95% CI of geometric mean (n = 10 CC rOMV-vaccinated mice) (*$p < 0.0001$). (B and C) Mortality (B) and weight loss (C) of mice challenged with a lethal dose (100 FFU) of influenza A/PR8 (n = 5 CC rOMV vaccinated, n = 5 PBS vaccinated, n = 5 pre-exposed). Kaplan-Meier survival curves were analyzed with a log-rank test. Error bars on morbidity curves represent SEM. (D) Total IgG and isotypes IgG1 and IgG2a titers of DBA/2J mice 8 weeks post-prime rOMV vaccination. Dotted line indicates lowest titer detectable above background. Log-transformed IgG1 and IgG2c titers compared using paired t test. Error bars indicate 95% CI of geometric mean (n = 5 CC rOMV-vaccinated mice) (*$p < 0.0001$). (E and F) Mortality (E) and morbidity (F) of DBA/2J mice challenged with a lethal dose (5,000 PFU, ~2.5 × LD_{50}) of influenza A/X-47 (n = 5 CC rOMV vaccinated, n = 5 PBS vaccinated). Kaplan-Meier survival curves were analyzed with a log-rank test. Error bars on morbidity curves represent SEM.

(Figure 5C). The 100% protection of C57BL/6 mice from challenge demonstrates the versatility of the CC M2e4xHet rOMV vaccine in protecting mice of different genetic background from influenza A/PR8 challenge.

ClearColi M2e4xHet rOMVs Elicit Anti-M2e IgG Titers and Protect DBA/2J Mice in Lethal Influenza A/X-47 Challenge or H3N2

M2e is highly conserved among different influenza strains; thus, mice immunized with M2e4xHet rOMVs should be protected from different subtypes of influenza other than influenza A/PR8 (H1N1). To test the robustness of the M2e rOMV antigen, DBA/2J mice were immunized with CC M2e4xHet rOMVs or given a PBS sham injection. DBA/2J mice are Th2 biased and share the same $H2^d$ major histocompatibility complex (MHC) as BALB/c mice, but are significantly more susceptible to many influenza types, allowing a lethal challenge to be performed using influenza A/X-47 (H3N2), which is typically only sublethal in BALB/c and C57BL/6 mice.[42,43] DBA/2J mice vaccinated with CC M2e4xHet rOMVs developed high levels of anti-M2e IgG titers and had a balanced IgG2a:IgG1 titer ratio, just as occurred in CC M2e4xHet rOMV-immunized BALB/c mice (Figure 5D). Following challenge with 5,000 plaque-forming units (PFU) of influenza A/X-47, 100% (five of five) of M2e4xHet rOMV-vaccinated DBA/2J mice survived—although they did experience ~10% weight loss—and 100% (five of five) of PBS sham-injected mice required euthanasia (Figures 5E and 5F). Thus, the survival of mice in X-47 challenge demonstrates that M2e4xHet rOMVs are effective at immunizing mice against influenza A strains of different subtypes.

ClearColi M2e4xHet rOMVs Elicit Anti-M2e IgG Titers in Ferrets and Reduce Virus Load in Lungs

The mouse studies indicated that M2e4xHet CC rOMVs showed promise as an influenza vaccine; thus, the vaccine was next evaluated in a more clinically relevant influenza animal model: ferrets. Unlike mice, which typically require influenza strains to be mouse adapted, ferrets are naturally susceptible to both human and avian influenza viruses. Additionally, ferrets infected with influenza present with fever, sneezing, and nasal discharge in addition to weight loss, more closely mimicking a human infection.[44] Three cohorts of six ferrets were immunized with either CC M2e4xHet rOMVs, CC "mock"

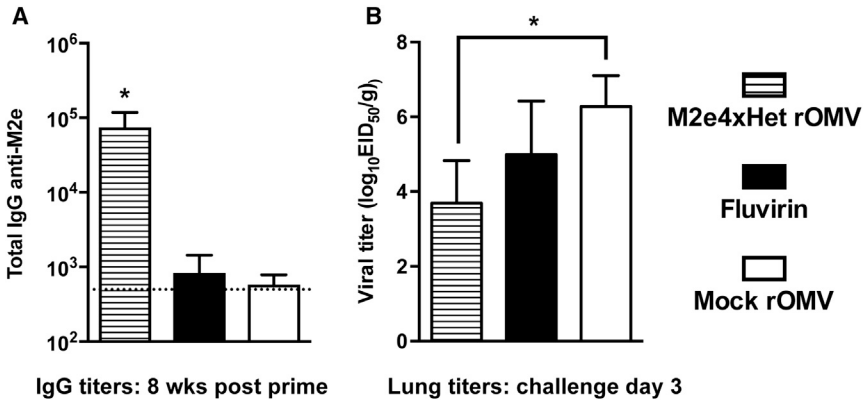

Figure 6. Ferret Antibody Titers and Lung Viral Titer Resulting from ClyA-M2e4xHet rOMVs Immunization

(A) Total IgG anti-M2e titers of ferrets 8 weeks post-prime vaccination. Error bars indicate 95% CI of geometric mean (n = 6 ferrets per group) (*$p < 0.01$). (B) Lung viral titers of ferrets 3 days post-challenge with influenza strain pdmH1N1 (n = 3 ferrets per group). Lung titers compared using ANOVA followed by comparison to mock CC rOMVs using Bonferroni method of correction (n = 3). Error bars indicate SD of log-transformed egg infectious dose (EID_{50}) per gram of lung tissue (*$p < 0.01$).

rOMVs (produced from *E. coli* that did not contain the pBAD ClyA-M2e4xHet encoding plasmid), or Fluvirin (a Food and Drug Administration [FDA]-approved seasonal influenza vaccine). Similar to the mouse experiments, the prime and boost doses were given 4 weeks apart, and blood was analyzed on day 56 (pre-challenge) to quantify antibody titers. Following each round of vaccinations, ferret body temperature was recorded to watch for fever, and injection sites were monitored for inflammation. None of the ferrets experienced any elevated temperature or injection site inflammation following the prime round of vaccination. Day 1 following the boost dose, six of six ferrets receiving the mock rOMV vaccine and six of six ferrets receiving the M2e4xHet rOMV vaccine exhibited slight-to-moderate inflammation, as indicated by redness and swelling at the injection site. By day 3 post-boost dose, the injection sites had recovered to normal in six of six ferrets in the mock rOMV group and five of six ferrets in the M2e4xHet rOMV group. None of the ferrets in the Fluvirin group experienced any inflammation. None of the ferrets in any cohort exhibited elevated temperatures, except one ferret in the M2e4xHet rOMV group. This one ferret's body temperature rose from a baseline temperature of 39°C prior to vaccination to 40°C 1 day post-vaccination. Although these side effects are not desirable, all were transient and none caused the ferrets severe distress. IgG anti-M2e titers were assessed 8 weeks post-prime vaccination and showed that all M2e4xHet rOMV-immunized ferrets developed high titers, whereas mock rOMV- and Fluvirin-immunized ferrets had anti-M2e titers that were indistinguishable from pre-vaccination sera (Figure 6A). Fluvirin is produced by purifying surface antigens from inactivated influenza; HA and NA are the predominant proteins present, but it is expected that some M2 protein may be present as well. However, it is unsurprising that the ferrets that received Fluvirin did not develop anti-M2e titers, due to the low amount of M2 present and the immunodominant nature of HA. Ferrets were challenged with pandemic A/California/7/2009 virus (pdmH1N1) 9 weeks post-initial vaccination, and their body temperature and weight were monitored. Day 3 post-challenge, three ferrets from each group were euthanized, and lungs were removed to assess viral titers. Ferrets vaccinated with M2e4xHet rOMVs showed a significant ($p < 0.01$) two-log reduction in lung viral titer compared to ferrets vaccinated with mock rOMVs (Figure 6B). Nasal turbinates and tracheas were also excised and assessed for viral titers, but neither the M2e4xHet- nor Fluvirin-vaccinated ferrets had titers that were significantly reduced from mock rOMV-vaccinated ferrets (Figure S4A). There was no significant difference in weight loss (Figure S4B) or in temperature (Figure S4C) among the three ferret cohorts. Overall, the mild side effects, high antibody titers, and low viral lung titers that resulted from M2e4xHet rOMV ferret immunization provide further evidence that CC rOMVs are a viable adjuvant platform.

DISCUSSION

Lipid IVa containing *E. coli* strain ClearColi was successfully engineered through genetic knockout to increase rOMV production. The CC-derived rOMVs offer a clear advantage over Nsl rOMVs in terms of their safety profile, as indicated by their reduced pyrogenicity in vitro and substantial attenuation of negative side effects in vivo. Although CC was developed to simplify the process of producing endotoxin-free proteins, CC rOMVs are still sufficiently immunogenic to serve as a potent adjuvant platform. Furthermore, the ability of CC rOMVs to adjuvant the immune response is applicable to both peptide-scale antigens, such as M2e4xHet (11.5 kDa), and protein-scale antigens, such as GFP (27 kDa). Both constructs led to high IgG titers that were equivalent to those generated by GFP in BL21-derived rOMVs. This work highlights the improved safety and versatility of the CC rOMV platform, greatly increasing its potential for use in larger animal systems.

One metric used to assess the safety of the CC rOMV platform was a pyrogenicity analysis using human whole blood. Traditionally, a limulus amebocyte lysate (LAL) assay is used to assess endotoxin in samples; however, this assay is not sensitive to the reduced toxicity of different lipid A acylation patterns, or to pyrogens other than endotoxin, making it unsuitable for assessing CC rOMV-associated toxicity.[45] The rabbit endotoxicity test is also standard, but for these translationally minded studies it was deemed more clinically relevant to use human blood samples in lieu of rabbits. The United States Pharmacopoeia recommends a maximum endotoxin level of 5 EU/kg for most drugs, which is the highest dose of endotoxin that does not elicit fever in humans or rabbits; however, vaccines are exempt from this clause.[46] The endotoxin unit levels associated

with specific vaccines are not widely reported, although one paper has extrapolated endotoxin units per milliliter levels of vaccines to show that some vaccines exceed this threshold; the typhus vaccine has about 800 EU/kg, and the typhoid vaccine has 8,000 EU/kg.[47] The BALB/c mice weighed approximately 20 g when given their prime vaccination, which, given the data in Figure 2A, corresponds to ~600 EU/kg, or 120 EU/mL for a 40-μg CC rOMV dose. Thus, although the vaccines do contain significantly more endotoxin than allowable for a traditional drug, they are lower than several vaccines currently used in humans. Future testing will identify the minimal CC rOMV dose needed to elicit a protective effect in murine models, as well as other relevant animal models of infectious disease.

The TLR agonist analysis indicated that CC rOMVs strongly stimulated TLR2, suggesting that it is critical to the immunogenicity of CC rOMVs. Additionally, the TLR4 data highlighted that CC rOMVs stimulate murine TLR4, but not human TLR4. The degree to which lipid IVa stimulates mTLR4 remains under investigation, suggesting that the mouse studies should be interpreted with some caution, as the exact contribution of mTLR4 signaling to the overall immune response elicited is unknown.[48] However, the lack of weight loss following vaccination with CC rOMVs suggests that mTLR4 is being stimulated less by CC rOMVs than by Nsl rOMVs. Follow-up studies using a humanized TLR4 mouse model could perhaps better ascertain the impact of TLR4 signaling on the immune response to CC rOMVs, although the current humanized TLR4 mouse model is on the Th1-biased C57BL/6 background.[49] Further work using murine TLR2, TLR4, and TLR2/4 knockout models will help to better define the mechanisms of adjuvant activity by CC rOMVs. Also interesting was that neither NOD1 nor NOD2, which both detect PAMPS located in peptidoglycan, were stimulated by CC rOMVs. Thus, although rOMVs derived from some pathogens, such as *Helicobacter pylori*, strongly stimulate NOD1, none of the *E. coli*-derived rOMVs tested induced response through NODs, suggesting that NOD1/2 are unlikely to account for the in vivo response elicited by the rOMV vaccine.[50] Overall, CC rOMVS appear to stimulate primarily through TLR2 stimulation, although future work can help to address other—and perhaps synergistic—signaling that may be occurring.

BALB/c, C57BL/6, and DBA/2J mice generated high IgG titers when vaccinated with CC rOMVs. That BALB/c mice vaccinated with CC rOMVs developed equivalent total IgG anti-M2e titers to Nsl rOMV-vaccinated mice is somewhat surprising, given the attenuated mTLR4 signaling and lack of TLR5 signaling from the CC rOMVs. However, previous work has demonstrated that TLR2 stimulation alone is sufficient to drive high anti-M2e titers in mice.[51] Additionally, the in vitro DC work reported here demonstrated that similar levels of mature DCs are produced following CC or Nsl rOMV stimulation. Thus, although CC rOMVs contain a slightly less diverse PRR profile than Nsl rOMVs, they still are effective at generating high IgG titers.

All BALB/c and C57BL/6 CC rOMV-immunized mice survived PR8 challenge, although the C57BL/6 mice experienced greater weight loss than the BALB/c-vaccinated mice after exposure to PR8. Although the IgG2c titers developed by C57BL/6 mice were equivalent to the IgG2a titers developed by BALB/c mice, C57BL/6 mice had significantly lower IgG1 titers. It is possible that the higher dose of influenza required for the C57BL/6 mice affected the response, or that there was a difference in T cell response. Wolf et al. produced multi-antigenic peptide influenza vaccines composed of four M2e peptides and two T helper cell epitopes adjuvanted with either CpG DNA or cholera toxin that elicited a robust antibody response in BALB/c mice, but not C57BL/6 mice, which they attributed to a lack of T cell responsiveness.[52] Although some controversy remains, C57BL/6 mice should be capable of generating potent anti-M2e antibodies; Rosendahl Huber et al. demonstrated the capability of C57BL/6 mice to develop weak titers against M2e when vaccinated using a M2e-based peptide vaccine adjuvanted with incomplete Freund's adjuvant and CpG DNA, although there was no difference in weight loss between vaccinated and non-vaccinated mice when challenged with influenza A virus X31.[53] Lee et al. found that M2e VLP particles supplemented with AS04 were sufficient to elicit protection in C57BL/6 mice against PR8 challenge, but that supplementation with monophosphoryl lipid A (MPL) or alum was not sufficient.[54] Using the CC rOMV vaccine, protection against PR8 influenza challenge in BALB/c and C57BL/6 mice and X-47 influenza challenge in DBA/2J mice was elicited without addition of any supplemental adjuvants (i.e., alum, CpG DNA). X-47 is a reassortant virus composed of the hemagglutinin and neuraminidase from A/Victoria/3/1975 and all other proteins from PR8; thus, the M2 protein is the same in both X-47 and PR8 virions, making it unsurprising that the CC M2e4xHet rOMV vaccine was effective against both X-47 and PR8.[55] Future work will further investigate the ability of CC M2e4xHet rOMVs to protect against influenza A strains with more divergent M2e peptides. Overall, the ability of CC rOMVs to protect mice of different genetic backgrounds from different influenza subtypes highlights the robustness of the CC rOMV adjuvant platform.

The ferret study further demonstrates that CC rOMVs remain immunogenic, even when used in a different animal model. Although the ferret model is frequently used for influenza vaccine trials, no literature to our knowledge has yet examined the interaction of lipid IVa with ferret TLR4, making it difficult to determine the degree to which TLR4 signaling is playing a role in the immune response to CC rOMVs. The literature further emphasizes the variability of lipid IVa signaling by species—it is a weak agonist of equine TLR4, but an antagonist in canine TLR4.[56] Further studies into the response of ferrets to lipid IVa will help us to better evaluate the immunogenicity of CC rOMVs in humans.

The ferrets that received the CC M2e4xHet rOMVs had statistically significant reduced viral lung titers compared to CC mock rOMVs, whereas ferrets that received Fluvirin had reduced—but not statistically significantly reduced—viral lung titers compared to CC mock rOMVs. This result is of special interest because one of the three HA variants that Fluvirin contains, derived from virus A/Christchurch/16/2010, is extremely similar to the HA in pdmH1N1, and

leads to neutralizing antibodies being formed that are effective against pandemic (pdm) H1N1.[57] Thus, the M2e4xHet CC rOMV vaccine did a better job at controlling influenza infection at day 3 post-challenge than the FDA-approved Fluvirin vaccine designed to generate neutralizing titers against the challenge pdmH1N1 virus. Although the ferrets that received CC rOMVs had reduced viral lung titers, they did exhibit weight loss in response to influenza challenge. Because antibodies against M2e are believed to drive protection through antibody dependent cellular cytotoxicity, not viral neutralization, as Fluvirin does, some weight loss is unsurprising.[35,58] Further work challenging ferrets with different flu subtypes will provide a better assessment of CC-rOMVs as a pandemic influenza vaccine. Additionally, a dosing study is necessary to determine the optimal CC M2e4xHet rOMV dose size for the ferrets. In another recent study involving an M2e-VLP platform, Music et al. found no difference in weight loss or in nasal viral titers between M2e-VLP-vaccinated ferrets and naive ferrets; however, they did not check the viral titers of the lungs, precluding a direct comparison with our results.[59] Interestingly, when Music et al. then supplemented their M2e-VLPs with a seasonal flu vaccine, this combination led to a reduction in both weight loss and viral titers following challenge. Thus, future work could examine the possibility of combining M2e CC-rOMVs with other influenza vaccines. Overall, the reduction of viral lung titers in CC rOMV-vaccinated ferrets indicates that the CC-rOMVs warrant further investigation as an influenza vaccine platform.

CC rOMVs represent a viable new adjuvant platform that offers benefits to current rOMV platforms. CC rOMVs retain the positive aspects of the rOMV vaccine platform—simple to produce, inexpensive, highly pathogen mimetic—but contain only the lipid IVa portion of LPS, giving them significantly greater translational potential than other available rOMV platforms. Even without a strong Th1 bias, CC rOMVs still elicit a robust humoral response. Furthermore, vaccination with CC M2e4xHet-rOMVs elicited complete protection of mice in a lethal influenza challenge against mouse strains with different MHC haplotypes and reduced lung viral titers in ferrets challenged with human pdmH1N1 influenza. Although CC rOMVs certainly hold promise in influenza vaccine development, this versatile platform has the potential for use in vaccines against a range of pathogens and offers a viable alternative to alum-based adjuvants.

MATERIALS AND METHODS

Strain Engineering to Induce Hypervesiculation

Hypervesiculating, *nlpI* knockout *E. coli* strains were constructed using phage transduction and the KeiO collection as previously described.[60,61] Briefly, *E. coli* donor strain MC4100 Δ*nlpI* kan^r was subcultured 1:100, then infected with P1 phage for 6 hr. Phage was collected and used to infect ClearColi (Lucigen) and BL21(DE3) (New England Biolabs) for 1.5 hr. Bacteria were centrifuged and plated on kanamycin (50 μg/mL) plates to select for *ΔnlpI* knockouts. Gene knockout was confirmed via PCR using primers nlpI-F and nlpI-R (Table S1) followed by sequencing and analysis using BLAST. To ensure strain contamination had not occurred during the knockout process, ClearColi *ΔnlpI* was sequenced with gutQ-F and gutQ-R to verify the absence of gene *gutQ* (Table S1).[17]

Recombinant OMV Production and Characterization

E. coli strains CC and BL21 were transformed with a pBAD plasmid expressing ClyA-GFP, as described by Kim et al.[5] *E. coli* strains CC and Nsl were transformed with a pBAD plasmid expressing ClyA-M2e4xHet, as described by Rappazzo et al.[10] Transformed strains were grown overnight (ON) in LB broth (Thermo Fisher Scientific) at 37°C, and then subcultured to OD_{600} = 0.08. Strains were induced with 2% L-arabinose (Sigma-Aldrich) at OD_{600} = 0.55 and grown for 18 more hours. Subsequently, bacteria were centrifuged (4°C, 15 min, 5,000 rcf) and passed through a 0.2-μm filter. The filtrate was ultracentrifuged (26,000 rpm, 4°C, 3 hr), then decanted, and the pellets suspended in sterile PBS. rOMV samples were aliquoted and stored at −20°C until use. rOMV surface protein content was determined using a BCA assay (Thermo Fisher Pierce), and antigenic content was determined via western blot (WB). To detect ClyA-GFP, polyclonal anti-GFP antibody was used (Life Technologies), and to detect ClyA-M2e4xHet, anti-His (clone HIS-1) antibody (Sigma-Aldrich) was used. WBs were developed using chemiluminescence and imaged with ChemiDoc Touch Imaging System (Bio-Rad). Semiquantitative analysis of WB demonstrated that 2% of total protein in Cly-GFP rOMVs was GFP and that ~6% of total protein in ClyA-M2e4xHet rOMVs was M2e4xHet (Figures S1A and S1B). TEM samples were prepared by negatively staining with 2% uranyl acetate on copper grids then imaged with a FEI T12 Spirit TEM.

Whole-Blood Pyrogen Testing

The protocol for the pyrogen test was adapted from Daneshian et al.[20] Donor blood was collected into a heparinized tube and rotated at room temperature until use (maximum time did not exceed 2 hr). Endotoxin-free 96-well tissue culture plates were filled with 200 μL of endotoxin-free saline, into which 20 μL of blood was added, along with 20 μL of rOMVs, 20 μL of lipid IVa (Carbosynth), or 20 μL of E-toxate endotoxin standard (Sigma-Aldrich). Endotoxin standard curve ranged from 10 to 0.125 EU/mL. Lipid IVa and rOMV samples were serially diluted by 10 (from 10 μg/mL to 0.001 pg/mL), plated in quadruplicate, and incubated (37°C, 18 hr). Subsequently, samples were centrifuged (500 rcf, 5 min, room temperature [RT]) and supernatant was collected. An IL-1β sandwich ELISA was performed on each supernatant, following the protocol from Biolegend. Plates were pre-coated with 2 μg/mL anti-IL-1β (clone H1b-27; Biolegend) in PBS overnight at 4°C. Plates were blocked (1% BSA, 1 hr, RT), incubated with 100 μL of supernatant per well (2 hr, 37°C), coated with anti-IL-1β biotin (clone H1b-98; Biolegend) (1 hr, RT), coated with avidin-HRP (Sigma-Aldrich) (30 min RT), and then developed with 3,3,5,5-tetramethylbenzidine (TMB) in the dark for 20 min. The reaction was stopped with 4N H_2SO_4, and absorbance was read at 450 nm. The plates were washed at least three times with wash buffer (0.3% bovine serum albumin plus 0.05% Tween 20 in PBS) between each step. A four-parameter logistic curve was fitted to the log of the endotoxin standard versus the standard absorbances using Prism6 software (GraphPad Software). All blood donors gave written,

informed consent, and the protocol for blood collection and use was approved by Cornell University's Institutional Review Board.

In Vitro Pathogen Recognition Receptor Studies

HEK-Blue KD-TLR5 cells (InvivoGen), which lack expression of all TLRs except TLR1 and TLR6, were transfected with individual human or mouse TLRs and stimulated with TLR ligands overnight, as previously described.[10] Cells were grown in complete DMEM media composed of the following: DMEM media (Corning), supplemented with 10 mM HEPES, 1 mM sodium pyruvate, 2 mM L-glutamine, 50 U/mL penicillin, 50 U/mL streptomycin, and 10% heat-inactivated low endotoxin fetal bovine serum (FBS) (VWR Life Science Seradigm). Subsequently, medium was assayed for secreted alkaline phosphatase activity using Quanti-blue (InvivoGen). Twenty microliters of each sample was added to 200 μL of Quanti-blue, incubated (37°C, 3 hr), and then read at absorbance of 630 nm. For sensitive chemiluminescence assay, cells were transfected with the following: 5x NF-κB-luciferase reporter plasmid and either murine MD-2, murine CD14, and murine TLR4 plasmids (InvivoGen) or human MD-2, human CD14, and human TLR4 plasmids (InvivoGen). Cells were stimulated with ligands overnight, and lysed (Reporter Lysis 5× Buffer; Promega). Luciferase activity was quantified by addition of 100 μL of D-luciferin substrate to 20 μL of lysate and read using a Veritas luminometer (Promega). NOD signaling assays were carried out using HEK-Blue mNOD1 and mNOD2 reporter cells (InvivoGen). Cells were plated at 0.28×10^6 cells/mL (NOD1) or 0.23×10^6 cells/mL (NOD2) and incubated (37°C, 48 hr) with 10 μg/mL positive control (NOD1: γ-D-glutamyl-meso-diaminopilemic acid [iE-DAP], NOD2: muramyl dipeptide [MDP]; InvivoGen), negative control (PBS), and rOMVs (100 ng/mL). Supernatant was subsequently collected and analyzed using Quanti-blue (InvivoGen).

BMDC Isolation and Maturation

Methods for generating BMDCs were adapted from Lutz et al.[62] Femurs were harvested from three 12-week-old C57BL/6 mice and three 12-week-old BALB/c mice (The Jackson Laboratory) and subsequently kept separate throughout the culturing process. Femurs were flushed with RPMI 1640 media (Corning), and the resulting cell suspension was centrifuged ($400 \times g$, 5 min, 4°C) and resuspended two times using RPMI 1640 media. Cells were cultured in Petri dishes (Corning) at 1×10^6 cells/mL in RPMI 1640 media supplemented with 10% low endotoxin heat-inactivated FBS, 2 mM L-glutamine, 50 U/mL penicillin, 50 U/mL streptomycin, 50 nM 2-mercaptoethanol, and 20 ng/mL recombinant granulocyte macrophage colony-stimulating factor (GM-CSF) (R&D Systems). One-half of the media was removed and replaced with fresh media on days 3 and 6 post-harvest. On day 7, all non-adherent and loosely adherent cells were harvested and plated in six-well plates (Corning) (2 mL/plate), then dosed with 100 ng/mL CC or Nsl rOMVs, or 100 ng/mL LPS. Cells were harvested for flow cytometry staining 24 hr after dosing using 50 mM EDTA in PBS. Cells were Fc blocked (Mouse BD Fc Block; BD) and stained for viability (Ghost Dye Violet 510 viability dye; excitation [Ex]: 405; emission [Em]: 510) (15 min, 4°C, in dark). Next, cells were surface stained for CD11c (violetFluor 450; Ex: 405; Em: 450), CD86 (PE; Ex: 496; Em: 578), and MHCII (redFluor 710; Ex: 633–647; Em: 710) (Tonbo Biosciences) (30 min, 4°C, in dark). Cells were then fixed (10% formaldehyde, 15 min, 4°C, in dark), resuspended in 1% FBS in PBS, and analyzed using flow cytometry. Data were collected using a LSR II flow cytometer and analyzed with FCS Express. DCs were gated on live, $CD11c^{Hi}$ cells. Mature DCs were identified as $MHCII^{Hi}$, $CD86^{Hi}$ cells. Concentration of cytokines IL-12p70, IL-10, TNF-α, and IL-6 in sample supernatants was determined by ELISA kits according to manufacturer instructions (R&D Systems). To determine the amount of type 1 IFN in supernatant, L929-ISRE cells were plated at 1×10^5 cells/well in a 96-well plate using complete DMEM. Cells were allowed to settle overnight, and then medium was removed and replaced with 50 μL of either DC supernatant or complete DMEM with IFN standards. Cells were incubated with these samples for 4 hr, then supernatant was removed, cells were lysed (Reporter Lysis 5× Buffer; Promega), and luminescence was measured using same procedure as described above for the transfected HEK-Blue KD-TLR5 cells.

Mouse Immunization

For the GFP trial, 10-week-old female BALB/c mice bred at Cornell University were subcutaneously injected with a prime dose of 20 μg of ClyA-GFP CC rOMVs (n = 5), 20 μg of ClyA-GFP BL21 rOMVs (n = 5), or 100 μL of PBS (n = 3). All mice received a boost dose of the same composition as the prime dose 4 weeks later. For the influenza trials, 7-week-old female BALB/c, C57BL/6, and DBA/2J mice (The Jackson Laboratory) were subcutaneously injected with 40 μg (total surface protein) of ClyA-M2e4xHet CC rOMVs in 100 μL of PBS (n = 11 BALB/c, n = 10 C57BL/6, n = 5 DBA/2J), 40 μg (total surface protein) of ClyA-M2e4xHet Nsl rOMVs in 100 μL of PBS (n = 12 BALB/c), or 100 μL of PBS (n = 16 BALB/c, n = 10 C57BL/6, n = 5 DBA/2J). Four weeks post-prime injection, a boost dose of the same composition was administered. All mice were weighed and observed daily following the prime (BALB/c, C57BL/6) and boost (BALB/c) injections. An additional cohort of mice, referred to as "pre-exposed," was immunized at age 8 weeks via intranasal injection of 5 FFU of influenza A/PR8 (n = 9 BALB/c, n = 8 C57BL/6) to give them immunity to the PR8 virus and allow them to serve as a positive vaccination control. All mouse work was approved by Cornell's Institutional Animal Care and Use Committee.

Enzyme-Linked Immunosorbent Assay

ELISAs were performed as previously described.[6,10] Briefly, Nunc Maxisorp plates (Nalge Nunc) were coated (2 μg/mL GFP, 12 hr, 4°C, or 2 μg/mL M2e peptide [SLLTEVETPIRNEWGSRSNDSSD] [LifeTein], 12 hr, 37°C), blocked (5% milk in PBS, 1 hr, 25°C), and then incubated with 2-fold serial dilutions of serum plated in triplicate (2 hr, 37°C). Plates were subsequently incubated with biotin-conjugated antibody (1:10,000 dilution; IgG, IgG1, or IgG2a) (eBiosciences) (1 hr, 37°C), incubated with HRP-avidin (1:10,000 dilution; 0.5 hr, 37°C), developed in the dark for 20 min with TMB (Thermo Fisher Scientific), and then stopped with 4N H_2SO_4, and absorbance was read at 450 nm. The plates were washed at least three times with wash buffer (0.3% bovine serum albumin plus 0.05% Tween 20 in

PBS) between each step. Titers were determined as the highest dilution in which the sample gave a signal greater than the average of naive serum at the same dilution plus three times the SD of the naive serum.

Mouse Influenza Challenge

Influenza A/Puerto Rico/8/1934 (PR8) virus (BEI Resources) was used to challenge BALB/c and C57BL/6 mice in the influenza vaccine trial. Previously, the PR8 stock was titered via fluorescent forming-units assay.[10] PR8 was diluted in PBS for use in exposure vaccination of the pre-exposed positive control mice and for use in the lethal challenges. All mice were challenged 10 weeks post their prime vaccination (for both subcutaneously injected and pre-exposed mice). Mice were administered 50 μL via intranasal injection of diluted PR8 while under isoflurane anesthesia (5 FFU for exposure vaccination of BALB/c and C57BL/6, 50 FFU for lethal challenge of BALB/c [$\sim 2.5 \times LD_{50}$], 100 FFU for lethal challenge of C57BL/6 [$\sim 2.5 \times LD_{50}$]). One hundred fluorescent forming units was selected for lethal challenge of C57BL/6 mice, as preliminary dosing studies indicated C57BL/6 mice were less sensitive than BALB/c to PR8. Influenza A virus reassortant X-47 (A/Victoria/3/1975 [HA, NA] × A/Puerto Rico/8/193 [H3N2]) (BEI Resources) was used to challenge DBA/2J mice. Virus was grown in embryonated eggs, then collected and titered via plaque-forming unit assay, as previously described.[63] Mice were weighed daily and observed twice daily following influenza infection. Any mouse with more than 30% weight loss, or exhibiting signs of severe distress, was humanely euthanized. All mouse work was approved by Cornell's Institutional Animal Care and Use Committee.

Ferret Immunization and Challenge

Three groups of six male Fitch ferrets (Triple F Farms) that were 7 months of age and serologically negative by hemagglutination inhibition (HI) for currently circulating influenza viruses were used for this study. Ferrets were housed in a Duo-Flo Bioclean Unit (Lab Products Incorporated) throughout the study and were intramuscularly vaccinated twice with either 500 μL (1.5 mg of total surface protein) of ClyA-M2e4xHet CC rOMV, 500 μL (1.5 mg of total surface protein) of CC rOMV that did not contain the pBAD plasmid (Mock-rOMV) or 500 μL of Fluvirin (2015–2016 formula; Norvartis Vaccines and Diagnostics Limited) at 4-week intervals for primary and boost vaccinations. Body temperature and local inflammation at the injection site (biceps femoris of caudal thigh) were monitored daily for 3 days post-vaccination. Serum samples were collected on day 28 (pre-boost) and on day 56 (pre-challenge) after primary vaccination for antibody titer determination. Ferrets were intranasally challenged 35 days after the boost vaccination with 1 mL of 10^6 PFU of A/California/7/2009 virus (pdmH1N1) virus diluted in PBS following anesthesia with ketamine-xylazine-atropine cocktail injection. Three ferrets from each group were observed daily for clinical signs of disease, weight loss, and lethargy as described previously.[64] The remaining three ferrets were euthanized on day 3 post-challenge (p.c.) so that nasal washes and respiratory tissues (nasal turbinate, trachea, and lung) could be collected to evaluate viral lung titers in the respiratory tract of ferrets by titrating samples in eggs. All animal experiments were performed under the guidance of the Centers for Disease Control and Prevention's Institutional Animal Care and Use Committee in an Association for Assessment and Accreditation of Laboratory Animal Care International-accredited facility.

Statistics

Groups in the pyrogenicity assay were compared with the Kruskal-Wallis test, followed by Mann-Whitney between pairs, using Bonferroni method to account for multiple comparisons. TLR/NOD signaling data, dendritic cell maturation marker data, cytokine production data, and mouse weight loss data were analyzed using an ANOVA, followed by multiple comparisons with respect to control using Dunnett's method of correction. Average titer values were calculated by taking the geometric mean of the titers in each cohort. IgG ELISA titer data were compared between two groups using a two-sided Student's t test on log-transformed data. IgG1 and IgG2a/IgG2c titer data were analyzed using a paired two-sided Student's t test on log-transformed data. Kaplan-Meier survival curves were analyzed with a log-rank test using a Bonferroni-corrected alpha to account for multiple comparisons. All statistical analyses were conducted using Prism6 software (GraphPad Software).

SUPPLEMENTAL INFORMATION

Supplemental Information includes four figures and one table and can be found with this article online at http://dx.doi.org/10.1016/j.ymthe.2017.01.010.

AUTHOR CONTRIBUTIONS

H.C.W. designed experiments, collected and analyzed data, and wrote the manuscript. C.G.R. designed experiments, collected and analyzed data, and assisted with editing the manuscript. J.S.H. designed experiments, collected and analyzed data, and assisted with writing the manuscript. X.S. assisted with experimental design, collected and analyzed data, and assisted with writing the manuscript. N.B., A.C., A.M., and J.P.B.C. collected and analyzed data and assisted with editing the manuscript. M.R.K. assisted with experimental design and with editing the manuscript. T.R.M. assisted with experimental design and with editing the manuscript. C.A.L. assisted with experimental design and analysis and with editing the manuscript. G.R.W. assisted with experimental design and analysis and edited the manuscript. M.P.D. contributed the paper concept and experimental design and edited the manuscript. D.P. contributed to experimental design and analysis and with editing manuscript.

ACKNOWLEDGMENTS

Funding for this work was provided through NIH Grant 1R56AI114793-01. This work made use of the Cornell Center for Materials Research Shared Facilities, which are supported through the NSF MRSEC Program (DMR-1120296). H.C.W. (Cornell University) was partially supported by a National Science Foundation Graduate Research Fellowship. Thank you to Jody Lopez (Cornell University College of Veterinary Medicine) for maintenance of the HEK-293 cell lines, Jeff Mattison (Cornell University) for blood collection,

Dorian LaTocha (Cornell University College of Veterinary Medicine) for assistance with flow cytometry, Dr. Erika Gruber (Cornell University College of Veterinary Medicine) for training in BMDC isolation, John Grazul (Cornell University) for assistance with TEM, Dr. Marco Straus (Cornell University College of Veterinary Medicine) for his assistance with the plaque formation unit assay, and Dr. Linxiao Chen and Dr. Jenny Baker (Cornell University) for their early discussions on the potential of ClearColi as a method for rOMV detoxification.

The findings and conclusions in this report are those of the authors and do not necessarily represent the views of the Centers for Disease Control and Prevention or the Agency for Toxic Substances and Disease Registry.

REFERENCES

1. Reed, S.G., Orr, M.T., and Fox, C.B. (2013). Key roles of adjuvants in modern vaccines. Nat. Med. *19*, 1597–1608.
2. Azmi, F., Ahmad Fuaad, A.A., Skwarczynski, M., and Toth, I. (2014). Recent progress in adjuvant discovery for peptide-based subunit vaccines. Hum. Vaccin. Immunother. *10*, 778–796.
3. Kuehn, M.J., and Kesty, N.C. (2005). Bacterial outer membrane vesicles and the host-pathogen interaction. Genes Dev. *19*, 2645–2655.
4. MacDonald, I.A., and Kuehn, M.J. (2012). Offense and defense: microbial membrane vesicles play both ways. Res. Microbiol. *163*, 607–618.
5. Kim, J.Y., Doody, A.M., Chen, D.J., Cremona, G.H., Shuler, M.L., Putnam, D., and DeLisa, M.P. (2008). Engineered bacterial outer membrane vesicles with enhanced functionality. J. Mol. Biol. *380*, 51–66.
6. Rosenthal, J.A., Huang, C.J., Doody, A.M., Leung, T., Mineta, K., Feng, D.D., Wayne, E.C., Nishimura, N., Leifer, C., DeLisa, M.P., et al. (2014). Mechanistic insight into the TH1-biased immune response to recombinant subunit vaccines delivered by probiotic bacteria-derived outer membrane vesicles. PLoS One *9*, e112802.
7. Chen, D.J., Osterrieder, N., Metzger, S.M., Buckles, E., Doody, A.M., DeLisa, M.P., and Putnam, D. (2010). Delivery of foreign antigens by engineered outer membrane vesicle vaccines. Proc. Natl. Acad. Sci. USA *107*, 3099–3104.
8. Baker, J.L., Chen, L., Rosenthal, J.A., Putnam, D., and DeLisa, M.P. (2014). Microbial biosynthesis of designer outer membrane vesicles. Curr. Opin. Biotechnol. *29*, 76–84.
9. Kaparakis-Liaskos, M., and Ferrero, R.L. (2015). Immune modulation by bacterial outer membrane vesicles. Nat. Rev. Immunol. *15*, 375–387.
10. Rappazzo, C.G., Watkins, H.C., Guarino, C.M., Chau, A., Lopez, J.L., DeLisa, M.P., Leifer, C.A., Whittaker, G.R., and Putnam, D. (2016). Recombinant M2e outer membrane vesicle vaccines protect against lethal influenza A challenge in BALB/c mice. Vaccine *34*, 1252–1258.
11. Kim, O.Y., Hong, B.S., Park, K.S., Yoon, Y.J., Choi, S.J., Lee, W.H., Roh, T.Y., Lötvall, J., Kim, Y.K., and Gho, Y.S. (2013). Immunization with *Escherichia coli* outer membrane vesicles protects bacteria-induced lethality via Th1 and Th17 cell responses. J. Immunol. *190*, 4092–4102.
12. Copeland, S., Warren, H.S., Lowry, S.F., Calvano, S.E., and Remick, D.; Inflammation and the Host Response to Injury Investigators (2005). Acute inflammatory response to endotoxin in mice and humans. Clin. Diagn. Lab. Immunol. *12*, 60–67.
13. Kim, S.H., Kim, K.S., Lee, S.R., Kim, E., Kim, M.S., Lee, E.Y., Gho, Y.S., Kim, J.W., Bishop, R.E., and Chang, K.T. (2009). Structural modifications of outer membrane vesicles to refine them as vaccine delivery vehicles. Biochim. Biophys. Acta *1788*, 2150–2159.
14. Chen, L., Valentine, J.L., Huang, C.-J., Endicott, C.E., Moeller, T.D., Rasmussen, J.A., Fletcher, J.R., Boll, J.M., Rosenthal, J.A., Dobruchowska, J., et al. (2016). Outer membrane vesicles displaying engineered glycotopes elicit protective antibodies. Proc. Natl. Acad. Sci. USA *113*, E3609–E3618.
15. Valentine, J.L., Chen, L., Perregaux, E.C., Weyant, K.B., Rosenthal, J.A., Heiss, C., Azadi, P., Fisher, A.C., Putnam, D., Moe, G.R., et al. (2016). Immunization with outer membrane vesicles displaying designer glycotopes yields class-switched, glycan-specific antibodies. Cell Chem. Biol. *23*, 655–665.
16. Hajjar, A.M., Ernst, R.K., Tsai, J.H., Wilson, C.B., and Miller, S.I. (2002). Human Toll-like receptor 4 recognizes host-specific LPS modifications. Nat. Immunol. *3*, 354–359.
17. Mamat, U., Wilke, K., Bramhill, D., Schromm, A.B., Lindner, B., Kohl, T.A., Corchero, J.L., Villaverde, A., Schaffer, L., Head, S.R., et al. (2015). Detoxifying *Escherichia coli* for endotoxin-free production of recombinant proteins. Microb. Cell Fact. *14*, 57.
18. Schwechheimer, C., Rodriguez, D.L., and Kuehn, M.J. (2015). NlpI-mediated modulation of outer membrane vesicle production through peptidoglycan dynamics in *Escherichia coli*. MicrobiologyOpen *4*, 375–389.
19. McBroom, A.J., Johnson, A.P., Vemulapalli, S., and Kuehn, M.J. (2006). Outer membrane vesicle production by *Escherichia coli* is independent of membrane instability. J. Bacteriol. *188*, 5385–5392.
20. Daneshian, M., von Aulock, S., and Hartung, T. (2009). Assessment of pyrogenic contaminations with validated human whole-blood assay. Nat. Protoc. *4*, 1709–1721.
21. Kajiwara, Y., Schiff, T., Voloudakis, G., Gama Sosa, M.A., Elder, G., Bozdagi, O., and Buxbaum, J.D. (2014). A critical role for human caspase-4 in endotoxin sensitivity. J. Immunol. *193*, 335–343.
22. Yoon, S.H., Han, M.J., Jeong, H., Lee, C.H., Xia, X.X., Lee, D.H., Shim, J.H., Lee, S.Y., Oh, T.K., and Kim, J.F. (2012). Comparative multi-omics systems analysis of *Escherichia coli* strains B and K-12. Genome Biol. *13*, R37.
23. Oblak, A., and Jerala, R. (2015). The molecular mechanism of species-specific recognition of lipopolysaccharides by the MD-2/TLR4 receptor complex. Mol. Immunol. *63*, 134–142.
24. Maeshima, N., and Fernandez, R.C. (2013). Recognition of lipid A variants by the TLR4-MD-2 receptor complex. Front. Cell. Infect. Microbiol. *3*, 3.
25. Franchi, L., McDonald, C., Kanneganti, T.D., Amer, A., and Núñez, G. (2006). Nucleotide-binding oligomerization domain-like receptors: intracellular pattern recognition molecules for pathogen detection and host defense. J. Immunol. *177*, 3507–3513.
26. Banchereau, J., and Steinman, R.M. (1998). Dendritic cells and the control of immunity. Nature *392*, 245–252.
27. Krummen, M., Balkow, S., Shen, L., Heinz, S., Loquai, C., Probst, H.-C., and Grabbe, S. (2010). Release of IL-12 by dendritic cells activated by TLR ligation is dependent on MyD88 signaling, whereas TRIF signaling is indispensable for TLR synergy. J. Leukoc. Biol. *88*, 189–199.
28. Netea, M.G., Van der Meer, J.W., Sutmuller, R.P., Adema, G.J., and Kullberg, B.J. (2005). From the Th1/Th2 paradigm towards a Toll-like receptor/T-helper bias. Antimicrob. Agents Chemother. *49*, 3991–3996.
29. Trinchieri, G. (2003). Interleukin-12 and the regulation of innate resistance and adaptive immunity. Nat. Rev. Immunol. *3*, 133–146.
30. Corinti, S., Albanesi, C., la Sala, A., Pastore, S., and Girolomoni, G. (2001). Regulatory activity of autocrine IL-10 on dendritic cell functions. J. Immunol. *166*, 4312–4318.
31. McNab, F., Mayer-Barber, K., Sher, A., Wack, A., and O'Garra, A. (2015). Type I interferons in infectious disease. Nat. Rev. Immunol. *15*, 87–103.
32. Trevejo, J.M., Marino, M.W., Philpott, N., Josien, R., Richards, E.C., Elkon, K.B., and Falck-Pedersen, E. (2001). TNF-α -dependent maturation of local dendritic cells is critical for activating the adaptive immune response to virus infection. Proc. Natl. Acad. Sci. USA *98*, 12162–12167.
33. Lehner, M., Kellert, B., Proff, J., Schmid, M.A., Diessenbacher, P., Ensser, A., Dörrie, J., Schaft, N., Leverkus, M., Kämpgen, E., and Holter, W. (2012). Autocrine TNF is critical for the survival of human dendritic cells by regulating BAK, BCL-2, and FLIPL. J. Immunol. *188*, 4810–4818.
34. Hunter, C.A., and Jones, S.A. (2015). IL-6 as a keystone cytokine in health and disease. Nat. Immunol. *16*, 448–457.
35. El Bakkouri, K., Descamps, F., De Filette, M., Smet, A., Festjens, E., Birkett, A., Van Rooijen, N., Verbeek, S., Fiers, W., and Saelens, X. (2011). Universal vaccine based on ectodomain of matrix protein 2 of influenza A: Fc receptors and alveolar macrophages mediate protection. J. Immunol. *186*, 1022–1031.

36. Schmitz, N., Beerli, R.R., Bauer, M., Jegerlehner, A., Dietmeier, K., Maudrich, M., Pumpens, P., Saudan, P., and Bachmann, M.F. (2012). Universal vaccine against influenza virus: linking TLR signaling to anti-viral protection. Eur. J. Immunol. *42*, 863–869.

37. Schotsaert, M., Ysenbaert, T., Neyt, K., Ibañez, L.I., Bogaert, P., Schepens, B., Lambrecht, B.N., Fiers, W., and Saelens, X. (2013). Natural and long-lasting cellular immune responses against influenza in the M2e-immune host. Mucosal Immunol. *6*, 276–287.

38. Kim, M.C., Song, J.M., O, E., Kwon, Y.M., Lee, Y.J., Compans, R.W., and Kang, S.M. (2013). Virus-like particles containing multiple M2 extracellular domains confer improved cross-protection against various subtypes of influenza virus. Mol. Ther. *21*, 485–492.

39. Zhou, D., Wu, T.L., Lasaro, M.O., Latimer, B.P., Parzych, E.M., Bian, A., Li, Y., Li, H., Erikson, J., Xiang, Z., and Ertl, H.C. (2010). A universal influenza A vaccine based on adenovirus expressing matrix-2 ectodomain and nucleoprotein protects mice from lethal challenge. Mol. Ther. *18*, 2182–2189.

40. Misplon, J.A., Lo, C.Y., Gabbard, J.D., Tompkins, S.M., and Epstein, S.L. (2010). Genetic control of immune responses to influenza A matrix 2 protein (M2). Vaccine *28*, 5817–5827.

41. Martin, R.M., Brady, J.L., and Lew, A.M. (1998). The need for IgG2c specific antiserum when isotyping antibodies from C57BL/6 and NOD mice. J. Immunol. Methods *212*, 187–192.

42. Sellers, R.S., Clifford, C.B., Treuting, P.M., and Brayton, C. (2012). Immunological variation between inbred laboratory mouse strains: points to consider in phenotyping genetically immunomodified mice. Vet. Pathol. *49*, 32–43.

43. Pica, N., Iyer, A., Ramos, I., Bouvier, N.M., Fernandez-Sesma, A., García-Sastre, A., Lowen, A.C., Palese, P., and Steel, J. (2011). The DBA.2 mouse is susceptible to disease following infection with a broad, but limited, range of influenza A and B viruses. J. Virol. *85*, 12825–12829.

44. Belser, J.A., Katz, J.M., and Tumpey, T.M. (2011). The ferret as a model organism to study influenza A virus infection. Dis. Model. Mech. *4*, 575–579.

45. Gutsmann, T., Howe, J., Zähringer, U., Garidel, P., Schromm, A.B., Koch, M.H.J., Fujimoto, Y., Fukase, K., Moriyon, I., Martínez-de-Tejada, G., and Brandenburg, K. (2010). Structural prerequisites for endotoxic activity in the Limulus test as compared to cytokine production in mononuclear cells. Innate Immun. *16*, 39–47.

46. Food and Drug Administration (2012). Guidance for Industry Pyrogen and Endotoxins Testing: Questions and Answers, *Vol. 1* (Food and Drug Administration), pp. 1–10.

47. Brito, L.A., and Singh, M. (2011). Acceptable levels of endotoxin in vaccine formulations during preclinical research. J. Pharm. Sci. *100*, 34–37.

48. Kolb, J.P., Casella, C.R., SenGupta, S., Chilton, P.M., and Mitchell, T.C. (2014). Type I interferon signaling contributes to the bias that Toll-like receptor 4 exhibits for signaling mediated by the adaptor protein TRIF. Sci. Signal. *7*, ra108.

49. Hajjar, A.M., Ernst, R.K., Fortuno, E.S., 3rd, Brasfield, A.S., Yam, C.S., Newlon, L.A., Kollmann, T.R., Miller, S.I., and Wilson, C.B. (2012). Humanized TLR4/MD-2 mice reveal LPS recognition differentially impacts susceptibility to *Yersinia pestis* and *Salmonella enterica*. PLoS Pathog. *8*, e1002963.

50. Irving, A.T., Mimuro, H., Kufer, T.A., Lo, C., Wheeler, R., Turner, L.J., Thomas, B.J., Malosse, C., Gantier, M.P., Casillas, L.N., et al. (2014). The immune receptor NOD1 and kinase RIP2 interact with bacterial peptidoglycan on early endosomes to promote autophagy and inflammatory signaling. Cell Host Microbe *15*, 623–635.

51. Zeng, W., Tan, A.C.L., Horrocks, K., and Jackson, D.C. (2015). A lipidated form of the extracellular domain of influenza M2 protein as a self-adjuvanting vaccine candidate. Vaccine *33*, 3526–3532.

52. Wolf, A.I., Mozdzanowska, K., Williams, K.L., Singer, D., Richter, M., Hoffmann, R., Caton, A.J., Otvos, L., and Erikson, J. (2011). Vaccination with M2e-based multiple antigenic peptides: characterization of the B cell response and protection efficacy in inbred and outbred mice. PLoS One *6*, e28445.

53. Rosendahl Huber, S.K., Camps, M.G.M., Jacobi, R.H.J., Mouthaan, J., van Dijken, H., van Beek, J., Ossendorp, F., and de Jonge, J. (2015). Synthetic long peptide influenza vaccine containing conserved T and B cell epitopes reduces viral load in lungs of mice and ferrets. PLoS One *10*, e0127969.

54. Lee, Y.N., Kim, M.C., Lee, Y.T., Hwang, H.S., Cho, M.K., Lee, J.S., Ko, E.J., Kwon, Y.M., and Kang, S.M. (2014). AS04-adjuvanted virus-like particles containing multiple M2 extracellular domains of influenza virus confer improved protection. Vaccine *32*, 4578–4585.

55. Baez, M., Palese, P., and Kilbourne, E.D. (1980). Gene composition of high-yielding influenza vaccine strains obtained by recombination. J. Infect. Dis. *141*, 362–365.

56. Scior, T., Alexander, C., and Zaehringer, U. (2013). Reviewing and identifying amino acids of human, murine, canine and equine TLR4 / MD-2 receptor complexes conferring endotoxic innate immunity activation by LPS/lipid A, or antagonistic effects by Eritoran, in contrast to species-dependent modulation by lipid IVa. Comput. Struct. Biotechnol. J. *5*, e201302012.

57. Community Network of Reference Laboratories (CNRL) for Human Influenza in Europe (2011). Influenza Virus Characterisation: Summary Europe, July 2011 (European Centre for Disease Prevention and Control).

58. Jegerlehner, A., Schmitz, N., Storni, T., and Bachmann, M.F. (2004). Influenza A vaccine based on the extracellular domain of M2: weak protection mediated via antibody-dependent NK cell activity. J. Immunol. *172*, 5598–5605.

59. Music, N., Reber, A.J., Kim, M.-C., York, I.A., and Kang, S.-M. (2016). Supplementation of H1N1pdm09 split vaccine with heterologous tandem repeat M2e5x virus-like particles confers improved cross-protection in ferrets. Vaccine *34*, 466–473.

60. Baba, T., Ara, T., Hasegawa, M., Takai, Y., Okumura, Y., Baba, M., Datsenko, K.A., Tomita, M., Wanner, B.L., and Mori, H. (2006). Construction of *Escherichia coli* K-12 in-frame, single-gene knockout mutants: the Keio collection. Mol. Syst. Biol. *2*, 2006.0008.

61. Thomason, L.C., Costantino, N., and Court, D.L. (2001). *E. coli* genome manipulation by P1 transduction. Curr. Protoc. Mol. Biol. *Chapter 1*. Unit 1.17.

62. Lutz, M.B., Kukutsch, N., Ogilvie, A.L.J., Rössner, S., Koch, F., Romani, N., and Schuler, G. (1999). An advanced culture method for generating large quantities of highly pure dendritic cells from mouse bone marrow. J. Immunol. Methods *223*, 77–92.

63. Costello, D.A., Whittaker, G.R., and Daniel, S. (2015). Variations in pH sensitivity, acid stability, and fusogenicity of three influenza virus H3 subtypes. J. Virol. *89*, 350–360.

64. Reuman, P.D., Keely, S., and Schiff, G.M. (1989). Assessment of signs of influenza illness in the ferret model. J. Virol. Methods *24*, 27–34.